fibers

MDPI

Article

Experimental Study on the Effect of Abaca Fibers on Reinforced Concrete: Evaluation of Workability, Mechanical, and Durability-Related Properties

Armando Arvizu-Montes [1,*], Stefany Alcivar-Bastidas [1,2] and María José Martínez-Echevarría [1]

[1] Department of Construction Engineering and Projects of Engineering, University of Granada, 18071 Granada, Spain; stefany.alcivar@cu.ucsg.edu.ec (S.A.-B.); mjmartinez@ugr.es (M.J.M.-E.)
[2] Facultad de Ingeniería, Universidad Católica de Santiago de Guayaquil, Guayaquil 090615, Ecuador
* Correspondence: aarvizu@ugr.es

Highlights

What are the main findings?

- The incorporation of abaca fibers did not compromise the fresh-state workability or mechanical properties while improving the flexural strength.
- Regarding durability, the presence of fibers influenced the corrosion intensity of the steel reinforcement, although no visible damage or deterioration was observed during the study period.

What is the implication of the main finding?

- Based on the observed durability results, service life estimations support the long-term performance of abaca-fiber-reinforced concrete.
- While the authors acknowledge further investigation to confirm long-term effects, the inclusion of abaca fibers demonstrated satisfactory performance in both fresh and hardened states, suggesting their potential as a reinforcement material for concrete.

Abstract: Interest in incorporating natural fibers as reinforcements in concrete has grown in parallel with the increasing need to reduce the environmental impact of construction. These fibers, known for their renewability, low cost, and life-cycle superiority, exhibit technical advantages such as light weight and high tensile strength. This study experimentally evaluated the influence of abaca fibers (AF) previously subjected to alkaline treatment and incorporated in reinforced concrete on workability, mechanical behavior, and durability, with a particular focus on the mechanisms affecting steel rebar corrosion. The characterization techniques included compressive and flexural testing; porosity, capillary water absorption, ion chloride penetration, and carbonation depth measurements; and corrosion rate monitoring via electrochemical methods. The results indicated that the addition of AF did not compromise the fresh-state properties or compressive strength but improved the flexural strength by 7.3%. Regarding durability, the porosity and water absorption increased by 4.1% and 8.2%, respectively, whereas the chloride penetration and carbonation depth remained within the requirements. Notable effects were observed regarding steel corrosion performance, where the incorporation of AF led to higher variability and an increasing trend in the corrosion rate compared with that of the reference concrete. Nevertheless, estimations suggest that abaca-fiber-reinforced concrete can meet the 100-year service life. These findings support the potential of AF as a viable reinforcement material for mechanical improvement; however, their influence on long-term durability, particularly corrosion, requires further investigation to deepen their feasible application for sustainable construction.

check for updates

Academic Editor: Hyun-Do Yun

Received: 15 April 2025
Revised: 8 May 2025
Accepted: 22 May 2025
Published: 4 June 2025

Citation: Arvizu-Montes, A.; Alcivar-Bastidas, S.; Martínez-Echevarría, M.J. Experimental Study on the Effect of Abaca Fibers on Reinforced Concrete: Evaluation of Workability, Mechanical, and Durability-Related Properties. *Fibers* **2025**, *13*, 75. https://doi.org/10.3390/fib13060075

Keywords: natural fibers; abaca fibers; self-compacting concrete; mechanical properties; durability; steel corrosion

1. Introduction

Concrete is one of the most frequently employed materials in civil engineering and construction, recognized for its cost-effectiveness and high compressive strength, among other properties. However, its performance under tensile stresses is well known to be limited [1,2]. To overcome this brittle behavior, one possible solution that has been extensively studied is the incorporation of randomly distributed fibers into the cementitious matrix, promoting a more ductile failure mode in the composite [3].

Natural fibers (NF) obtained from plants such as bamboo, jute, or sisal have seen a significant increase in use in the past few years, acting as effective reinforcements in composite materials [4,5]. Given their abundance, affordability, and eco-friendliness, the use of plant fibers in building materials has gained widespread attention worldwide, particularly within the scientific community. This trend is partly driven by the environmental impact of the construction industry, which is recognized as a major contributor to ecological damage on a global scale [6,7]. Furthermore, NF offer specific advantages that might enhance composite materials, including light weight, low cost, high tensile strength, and stiffness [8].

In contrast, industrial fibers, frequently based on steel and synthetic materials, are commonly employed in the construction sector [9], for instance, to improve the resistance and ductility of concrete elements [10]. However, the cost of producing these fibers is high, resulting in carbon dioxide emissions and the consumption of non-renewable resources [11]. Recent studies have demonstrated that certain properties of NF could match those of various types of industrial fibers, suggesting that with the incorporation of natural fibers, the "go green" necessity in the construction sector could be addressed by introducing more environmental materials and innovative technologies [12–14]. Previous studies on natural fibers, such as flax [15] or sisal [16], have shown promising results in cement composite applications, highlighting that the overall performance of NF can vary depending on different factors, including plant type, climate conditions, age, and processing methods [16].

Among the natural fibers explored by researchers, this study focuses on abaca fibers (AF). Extracted from the pseudo-stem of *Musa textilis*, also known as Manila hemp, abaca belongs to the Musaceae family (banana plants). These fibers are abundantly accessible in tropical nations such as the Philippines or Ecuador [17,18]. AF have been recognized by different authors as one of the strongest fiber types available in the realm of plant-based fibers [19,20], demonstrating promising results in terms of tensile strength, which reaches values between 410 and 810 MPa [21]. This indicates their potential in the construction industry for concrete reinforcement, improving flexural strength and representing a tentative alternative for replacing synthetic fibers [22].

Chemical and physical treatments have been explored by researchers seeking to increase the steadiness and performance of NF in cementitious materials [23]. These treatments are aimed at improving the fiber–matrix interface, addressing inadequate fiber distribution within the paste, and mitigating challenges related to moisture absorption and porosity [24–26]. Such modifications have demonstrated promising results, significantly enhancing both the mechanical and durability-related properties of cement-based materials, thereby increasing the overall performance of the composite [27,28].

Moreover, steel corrosion is widely recognized as a major challenge to the structural integrity of reinforced concrete elements, with rebar corrosion frequently highlighted as a significant factor in reducing their durability [29]. However, despite the importance of

this issue, there remains a lack of evidence on the effect of fibers on the corrosion process after being incorporated into cementitious matrices. While some studies on fiber-reinforced concrete have demonstrated comparable or even enhanced performance regarding corrosion resistance [27,30,31], concerns exist that an increase in porosity originating from the presence of NF might destabilize the passivation state of the embedded steel reinforcement, compromising the service life of the structure. Hence, a systematic understanding of how NF, particularly abaca fibers, influence the durability of reinforced concrete, especially in terms of rebar corrosion, is still lacking. This knowledge is essential for assessing the viability of using natural fibers in concrete structures.

The present study aims to evaluate the influence of natural fibers as reinforcement in concrete, seeking to explore their technical viability for potentially more sustainable practices. Self-compacting concrete incorporating abaca fibers was designed to assess their effect on rheological, mechanical, and durability properties, with a particular focus on the mechanisms that can affect the corrosion process of steel rebar. These were investigated through an experimental procedure analyzing workability in the fresh state, mechanical performance via compressive and flexural strength, and durability-related parameters, including porosity, water absorption, ion chloride penetration, carbonation depth, and direct measurements of the corrosion rate. A plain concrete mix was used as a reference to further identify the effects of the abaca fibers.

It is expected that the incorporation of AF into concrete will enhance its mechanical performance; however, the nature of the impact these fibers may have on the corrosion behavior of the steel reinforcement remains unclear, as the fibers may alter the inherent characteristics of the composites. In this line, the novelty of this study lies in the long-term monitoring of steel corrosion over one year using nondestructive electrochemical techniques, enabling an in-depth understanding of how natural fibers influence rebar corrosion behavior in concrete, a subject that remains underexplored in the current literature and is critical for evaluating the long-term performance of reinforced concrete.

2. Materials and Methods

An extensive experimental program was conducted to evaluate the influence of abaca fibers on concrete performance. The procedure involved incorporating 2.5 kg/m^3 of AF into the concrete mix design, designated as abaca-fiber-reinforced concrete (AFRC). This dosage was selected in accordance with the recommendations of the Spanish Code, which specifies a minimum fiber content of 0.25% by volume for fibers used with structural purpose [32]. Additionally, a reference reinforced concrete (RRC) without fibers served as a comparative baseline. The experimental procedure is detailed in the subsequent sections.

2.1. Materials

2.1.1. Abaca Fibers

The abaca fibers employed in this research were imported from Ecuador in their natural state, without undergoing any chemical or physical treatment. Previous studies have stated that the performance of fibers in cementitious composites is strongly influenced by parameters such as length, geometry, and content in the mix [33,34]. In this context, experimental results have suggested a length of 30 mm for optimal performance in cement composites using this particular AF [35], thus providing a basis for its selection in this study.

Following the procedures established by prior authors with natural fibers [27,28] and aiming to enhance their long-term durability in the cementitious matrix, AF were subjected to a chemical treatment prior to their inclusion in the mixture. To begin the process, the fibers were immersed in a 3% mass percentage NaOH solution for 4 h. Subsequently, they

were submerged in ordinary water for ten hours. Once the AF were soaked, water was used to wash them repeatedly until the water turned completely clear. To decrease the moisture absorption and enhance the stiffness of the fibers, they were dried in a furnace for 24 h at 85 ± 1 °C. Finally, the AF underwent cooling to reach room temperature and were hermetically preserved [35]. Figure 1 denotes the treatment process.

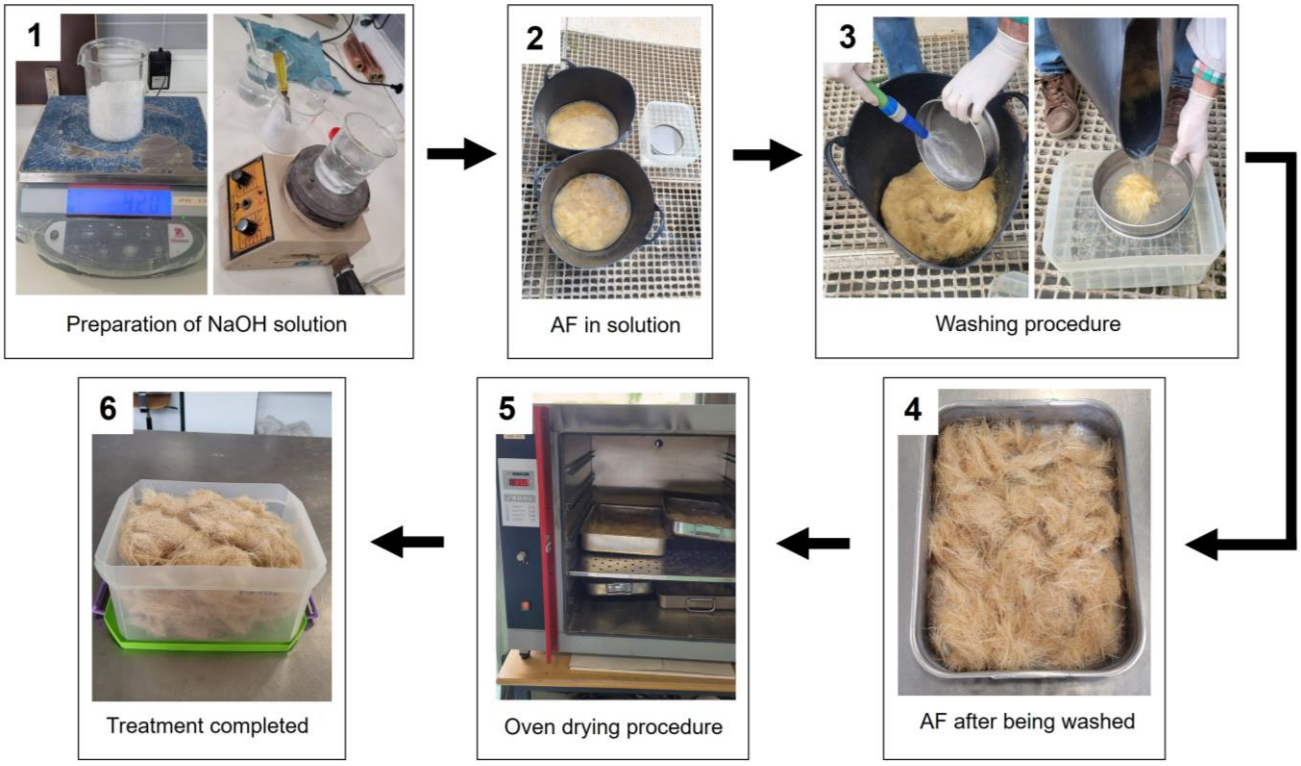

Figure 1. NaOH treatment applied to abaca fibers.

As reported by Alcivar-Bastidas et al. [35], the alkalinization of abaca fibers led to an increase in tensile strength and crystallinity of 36% and 26%, respectively. These improvements were attributed to the elimination of non-cellulosic components [35]. To further evaluate the effect of this treatment, Fourier transform infrared spectroscopy (FTIR) was performed to identify the functional groups in the fibers. Figure 2 shows the FTIR spectra of the untreated and treated AF, registered in absorbance over the range of 4000–750 cm^{-1}, before and after NaOH treatment. The main functional group assignments are presented in Table 1, according to several authors [36–38]. Furthermore, the spectra also demonstrate the elimination of peaks corresponding to hemicellulose and pectin (peaks at 1710 and 1520 cm^{-1}, respectively), validating their partial elimination after treatment and establishing the efficiency of the procedure.

Additionally, to examine the morphological changes induced by alkali treatment, scanning electron microscopy (SEM) analysis was conducted on the surfaces of the fibers before and after the treatment. As observed in Figure 3, the untreated AF present a smoother surface, whereas the treated fibers exhibit pronounced surface roughness. These topographical modifications increase the effective area available for contact with cement paste, enhancing the fiber–matrix interface and thereby improving mechanical performance of the composite, as stated by previous authors [39,40].

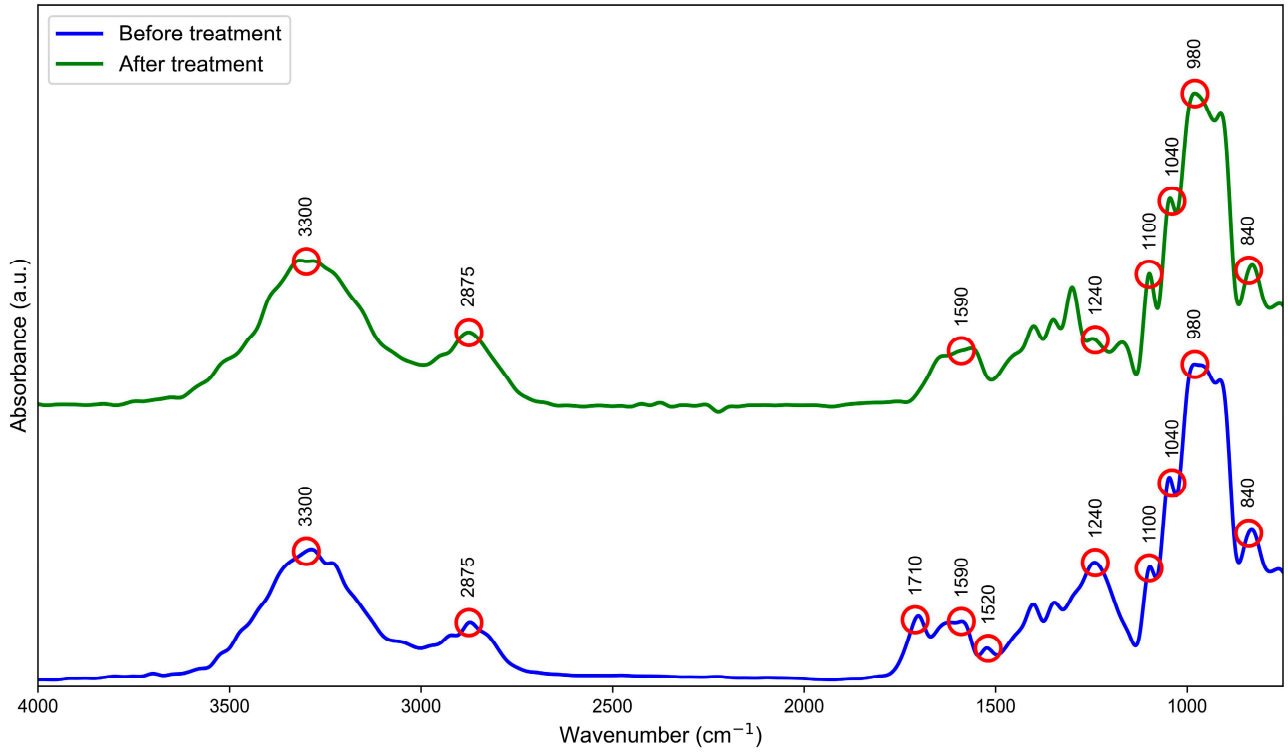

Figure 2. FTIR spectrograms for abaca fibers before and after alkaline treatment.

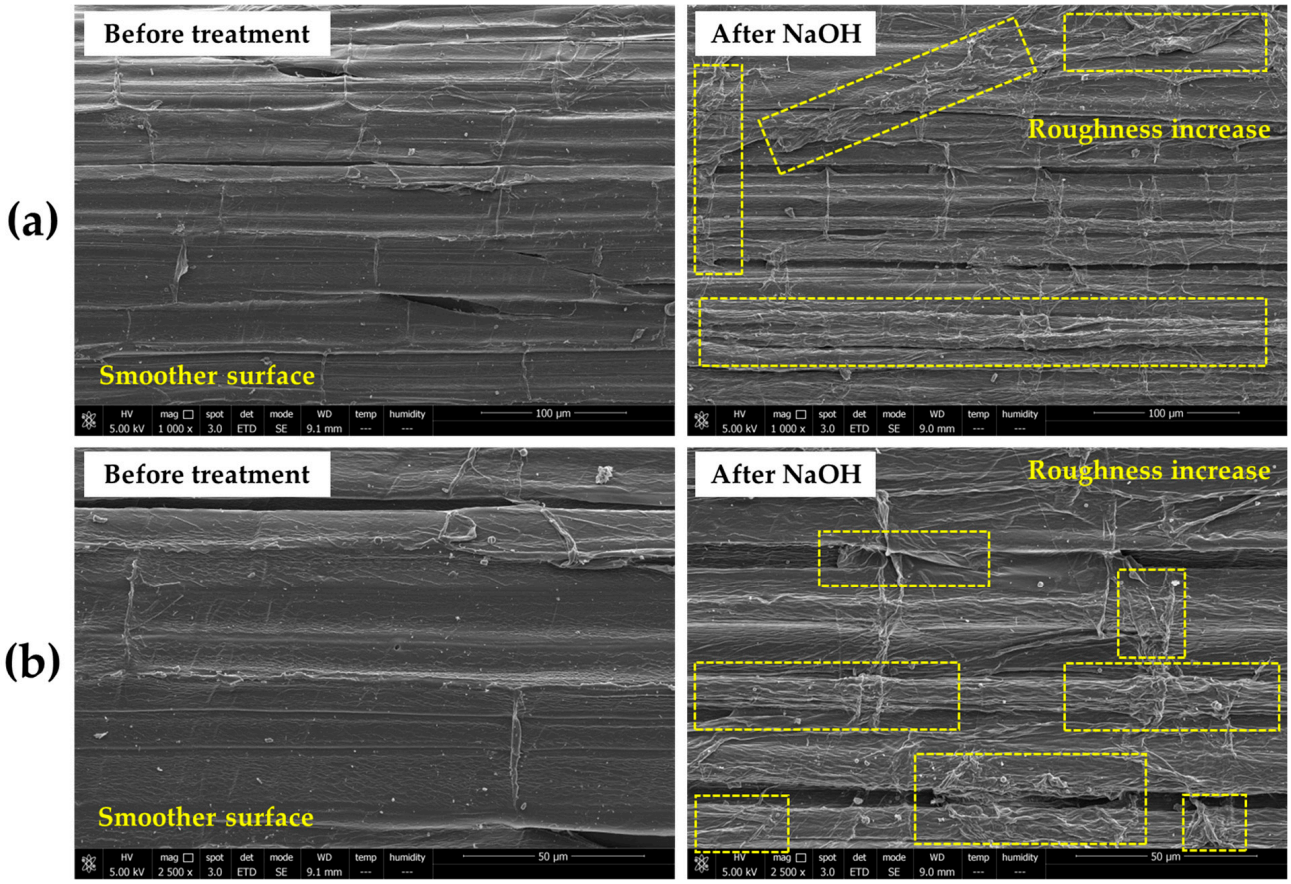

Figure 3. SEM images of abaca fibers before and after alkaline treatment: (**a**) 100 µm; (**b**) 50 µm.

Table 1. FTIR spectra data for abaca fibers.

Peak (cm^{-1})	Functional Group	Possible Assignment
3300	-OH	Cellulose, hemicellulose, and lignin
2875	C-H	Cellulose and hemicellulose
1710	C=O	Hemicellulose and pectin
1590	C=C	Lignin components
1520	C-H	Hemicellulose and pectin
1240	C-O	Lignin
1100	C-O-C	Cellulose
1040	C-O	Hemicellulose and lignin
980	Glycosidic links	Polysaccharide
840	C-OH	β-glycosidic linkages

Moreover, Table 2 summarizes the key physical and mechanical properties of the AF used in this study following NaOH treatment, providing relevant insights into their reinforcing behavior within cement-based materials.

Table 2. Properties of abaca fibers used in this study after NaOH treatment.

Length (mm)	Water Absorption (%)	Cross Section (mm^2)	Tensile Resistance (MPa)
30 ± 2	70.7 ± 5.3	0.04 ± 0.01	465.2 ± 31.4

2.1.2. Concrete

Considering the type of environmental exposure observed in Granada, Spain, and implementing the guidelines of Okamura and Ouchi [41] for self-compacting concrete (SCC), AFRC was dosed following the specifications established in the Spanish Code [32]. The materials used included Portland cement (CEM I 42.5 R-SR 3), in accordance with UNE-EN 197-1 [42], provided by "Cementos Portland Valderrivas", and, to enhance the workability [43], a crushed limestone–dolomitic filler with a density of 2830 kg/m^3, supplied by "Triturados Puerto Blanco" and sourced from local quarries in the zone of Granada, Spain.

The aggregates, also limestone–dolomitic in nature and acquired from the same supplier, were classified as natural sand (NS), natural medium gravel (NMG), and natural coarse gravel (NCG) with particle size of 0–4 mm, 4–8 mm, and 8–16 mm, respectively. Figure 4 shows their size distributions. The admixture used for this study was MasterEase 3530, a superplasticizer (SP) supplied by Master Builders Solutions, Barcelona, Spain.

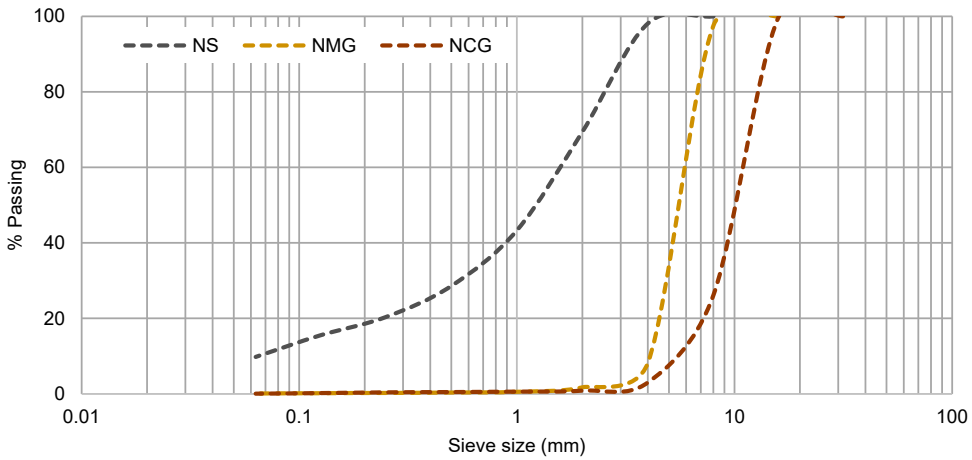

Figure 4. Particle size distribution curve of aggregates.

2.2. Methods

2.2.1. Mixture Proportions

To ensure a uniform distribution of the fibers in the mixture, a self-compacting concrete was designed, acknowledging that a key attribute of SCC is its flowability without external vibration [44] and particularly the capability to incorporate by-products in the mix without compromising its fresh properties [45]. Several trial batches were employed to establish the ideal composition, considering the content of fibers and ensuring compliance with SCC requirements. Additionally, to promote the dispersion of AF, these were incorporated in two phases during the mixing process: first, half of the fiber content was mixed with the aggregates in a dry state, and then a portion of the mixing water was added; subsequently, the rest of the fibers were gradually introduced to the cement, along with the remaining mixing water and superplasticizer. This approach, further aided by the workability of SCC, ensured the distribution of AF in the composite. The final dosage included 2.5 kg/m^3 of AF and a water/cement ratio of 0.55. The mix proportions, presented in Table 3, indicate that AFRC and RRC share identical component quantities, differing only in the incorporation of abaca fibers.

Table 3. Mixture proportions (kg/m^3).

	Water	**Cement**	**Filler**	**NS**	**NCG**	**NMG**	**SP**	**AF**
AFRC	165	300	173.5	680	536	536	6.6	2.5
RRC	165	300	173.5	680	536	536	6.6	-

2.2.2. Fresh-State Concrete Properties

After the adjustment of the dosage, considering the inherit variability of concrete, three batches of 40 L were prepared to determine the required parameters of self-compactability for each concrete. For the present study, according to the Spanish Code [32], the workability of fresh concrete was evaluated by the following tests: slump flow (UNE-EN 12350-8) [46], V-funnel (UNE-EN 12350-9) [47], J-ring (UNE-EN 12350-12) [48], and L-box (UNE-EN 12350-10) [49].

2.2.3. Hardened-State Concrete Properties

Further batches were cast to prepare the required test specimens to determine the parameters in the hardened state. After a 28-day curing period in a controlled humid chamber maintained at 20 ± 2 °C and 95 ± 2% relative humidity, compressive and flexural strength tests were conducted to evaluate the mechanical properties. The compressive strength was determined on 100 mm cubic samples according to UNE-EN 12390-3 [50] using a IBERTEST MOD. MEH-3000 PT-W testing machine. In contrast, flexural strength testing, in line with UNE-EN 12390-5 [51], was carried out with 100 × 100 × 400 mm prismatic samples, and the testing machine corresponded to the IBERTEST MOD. TESTRONIC-100-MD2.

Moreover, additional tests related to durability and corrosion mechanisms affecting steel reinforcements were conducted, considering both destructive and non-destructive electrochemical techniques. This approach is essential given the multiple factors influencing the corrosion process [52], as well as the challenge of identifying structural degradation in concrete elements before they begin to spall [53]. The procedures for these tests are detailed as follows:

- Accessible porosity for water and water absorption: The determination of these parameters followed the guidelines outlined in UNE 83980 [54] employing the boiling method on cubic samples (100 mm), considering three specimens per mixture in order to increase the reliability of the results.

- Water absorption by capillary action: This was assessed using 100 mm cubic specimens (previously conditioned as the standard indicates) in contact with a 5 mm water film. Weight gain was periodically measured in accordance with UNE 83982 [55] to calculate the coefficient of water absorbed by capillary action in hardened concrete. The respective coefficients were obtained by the method of least squares, fitting (i) the absorption measured during the first 6 h (initial absorption) and (ii) secondary absorption (longer period) to a straight line.
- Chloride ion penetration: The test was performed following the specifications in the ASTM C1202-25 [56] Standard, monitoring the electrical current through cylindrical samples (previously conditioned according to the norm) 100 mm in nominal diameter and 50 mm thick over a period of 6 h. A 60 V potential was applied between two containers, one with NaCl and the other with NaOH, to measure the charge passed (Qs) and assess concrete resistance to chloride ion penetration.
- Carbonation depth: Since the natural carbonation process progresses slowly, an accelerated carbonation test was conducted to evaluate this development, following the procedure described by UNE-EN 12390-12 [57]. The specimens, measuring 60 × 60 × 285 mm, remained in an accelerated carbonation chamber with a 1% CO_2 concentration at a temperature of 20 ± 2 °C and relative humidity of 57 ± 3% for a year. After the exposure time, and at other intermediate time points, a piece of concrete was broken in two parts, and a phenolphthalein solution was applied to the fractured zone. The carbonation depth corresponded to the mean length of the uncolored area on the surface, utilizing three different specimens for each type of concrete studied.
- Direct measurements of corrosion rate: The specimens utilized were standardized steel rebar classified as B 500 SD according to the Spanish Code [32], with a 12 mm diameter and a length of 220 mm. Four rebar samples were tested per concrete type, embedded in pairs within prismatic concrete specimens (20 × 20 × 8 cm) considering a cover of 30 mm. Following the methodology established in a previous work [29], the electrochemical measurements were conducted using a calomel reference electrode, with two AISI 304 stainless steel wires (Φ 3 mm) as counter electrodes placed parallel to the rebar, along with an additional pair of external counter electrodes. Figure 5 illustrates the experimental setup employed in detail. To monitor the corrosion potential and intensity of the steel rebar, the electrochemical resistance technique was employed [58]. Measurements were performed using a PARSTAT 2263 potentiostat (Princeton Applied Research, AMETEK, Hampshire, England). After applying a polarization of ±10 mV (ΔV), the necessary corrosion rate was measured (ΔI). The corrosion rate (I_{corr}) was then calculated as the mean value of three determinations following the equation proposed by Martinez-Echevarria et al. [59]:

$$I_{corr} = \frac{B}{Rp} \quad (1)$$

where

I_{corr} = corrosion rate.
B = constant of 26 mV, in agreement with earlier publications [60,61].
Rp = polarization resistance, evaluated as ΔV/ΔI.

Finally, i_{corr} was obtained by dividing the value of I_{corr} by the area of the steel surface (considered for this case as 55 cm^2) directly in contact with the concrete.

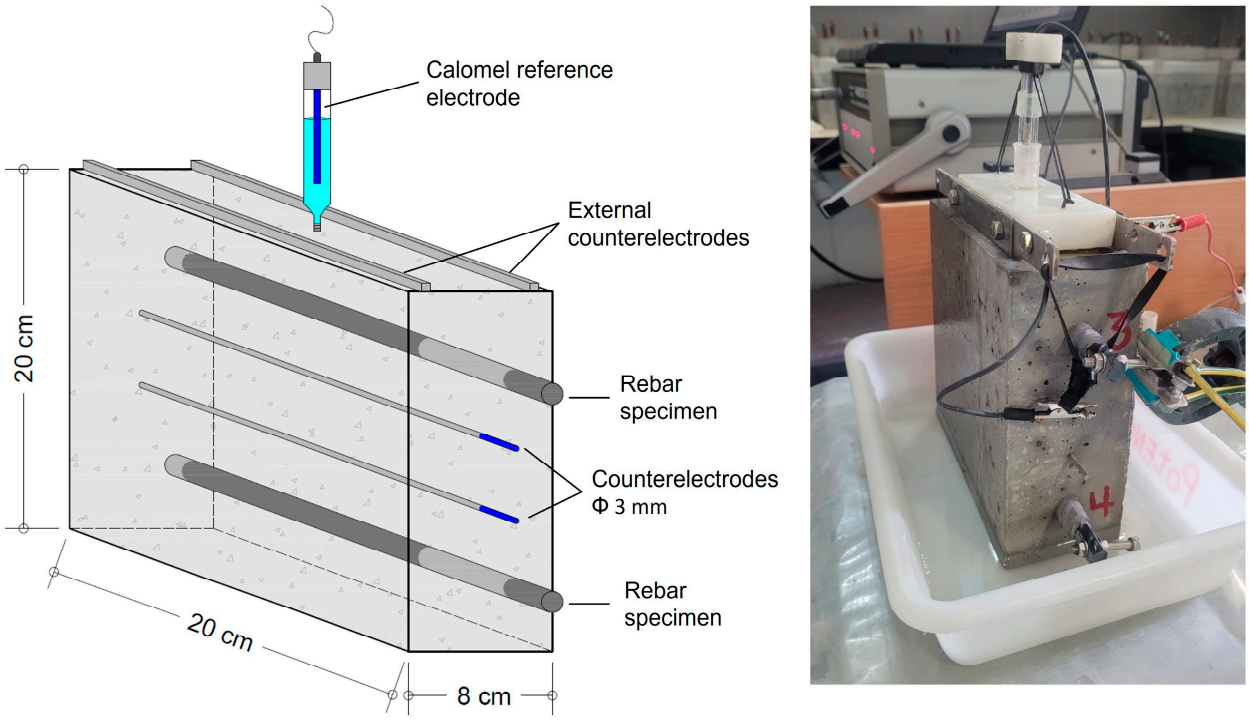

Figure 5. Set up for corrosion intensity measurements.

3. Results and Discussion

3.1. Workability in Fresh-State

Table 4 summarizes the results of the self-compactability tests, presenting the mean value from three batches per concrete type based on the previous established dosage, alongside the range parameters specified in the Spanish Code [32].

Table 4. Self-compactability test results.

	Slump Flow PJ (mm)	V-Funnel tv (s)	J-Ring PJ (mm)	L-Box PL
AFRC	770	18.2	9.5	0.8
RRC	760	17.1	9.0	1.0
Permissible range	550–850	≤25	≤10	≥0.80

Research has demonstrated that the inclusion of fibers affects the workability and flow of fresh concrete [62,63], with the effects depending on both the content and nature of the fibers. Nevertheless, previous studies have shown that SCC can still meet the required criteria, even when fibers modify its rheological parameters [64]. In this context, the incorporation of AF led to a slight modification of the SCC parameters, which was attributed to the hydrophilic nature of cellulosic fibers, which tend to absorb water from the mix, thereby reducing the amount of free water available for the flow of the mixture [65]. However, as observed in Table 4, considering the dosage used in this study, the presence of abaca fibers did not impede the achievement of the desired fresh properties. The AFRC achieved acceptable results in all conducted tests, in line with the limits established by the Spanish Code, thus demonstrating that workability was not compromised.

3.2. Mechanical Properties

After 28 days in the humid chamber, Table 5 presents the mechanical properties as the mean value of three specimens of different batches per parameter, along with their

corresponding standard deviation (SD) and coefficient of variation (CV). The dispersion obtained from these results was very low, further confirming the reliability and minimization of batch-to-batch variability.

Table 5. Mechanical properties at 28 days.

	Compressive Strength			Flexural Strength		
	MPa	**SD**	**CV (%)**	**MPa**	**SD**	**CV (%)**
AFRC	54.06	0.88	1.63	8.33	0.36	4.33
RRC	55.07	0.84	1.52	7.76	0.26	3.29

The abaca fibers used in this study were ineffective in improving the compressive strength. However, while other studies have indicated that the compressive resistance decreases with fiber incorporation in the cementitious matrix [66,67], the AFRC demonstrated acceptable resistance against compressive effects, only 1.8% under that of the RRC, indicating that this particular property remains barely unaffected by AF. Additionally, these outcomes are consistent with the considered w/c ratio and comparable to SCC resistances reported in the literature [68].

On the other hand, the flexural strength presented an increase of 7.3% compared to that of the reference concrete, as shown in Table 3. In this regard, the incorporation of fibers limits crack development within the composite by creating a bridging effect, enhancing flexural toughness, and preventing brittle failure [3]. Moreover, this flexural improvement has been also reported by recent researchers working with natural fibers as reinforcement in cement-based materials [69,70].

3.3. Durability-Related Properties

3.3.1. Porosity and Water Absorption

The porosity and water absorption results, obtained as the mean of three measurements per concrete type, are presented in Table 6. Research has highlighted that including fibers in cementitious mixtures increases the presence of larger pores in the matrix, leading to higher porosity and water absorption [71]. This effect can be further pronounced with natural plant fibers due to their inherently higher tendency to absorb water [72].

Table 6. Porosity and water absorption (after immersion and vacuum).

	Porosity		Water Absorption	
	(%)	**SD**	**(%)**	**SD**
AFRC	10.96	0.21	5.3	0.11
RRC	10.53	0.15	4.9	0.09

Nonetheless, the results indicate a minimal difference between both concretes. As shown in Table 4, the AFRC exhibits only a 4.1% increase in porosity compared to the RRC, leading to a corresponding rise in water absorption Moreover, when compared to similar self-compacting mixtures [73,74], the AFRC remains within an acceptable porosity range. It is worth noting that although porosity and water absorption are generally inversely related to mechanical performance, where lower porosity typically results in higher strength, this relationship does not necessarily apply to cementitious composites incorporating cellulosic fibers, as stated by Caixeta Silva et al. [75]. Alkaline treatments increase the crystallinity of the fibers, enhancing their interaction with the cement matrix and thereby improving the overall mechanical behavior, even in the case of a more porous material [75].

This supports the outcomes of the present study, where the observed increase in the porosity of the AFRC did not result in a reduction in the mechanical performance,

as previously discussed. Therefore, based on these findings, the addition of abaca fibers should not negatively affect the durability of concrete.

3.3.2. Water Absorption by Capillary Action

Figure 6 represents the water absorption by capillary action, related to the square of time. During the first six hours, AFRC exhibited a capillary absorption coefficient of 3.14 g/(m^2·s$^{0.5}$), which subsequently decreased to 1.10 g/(m^2·s$^{0.5}$). The corresponding coefficients are listed in Table 7.

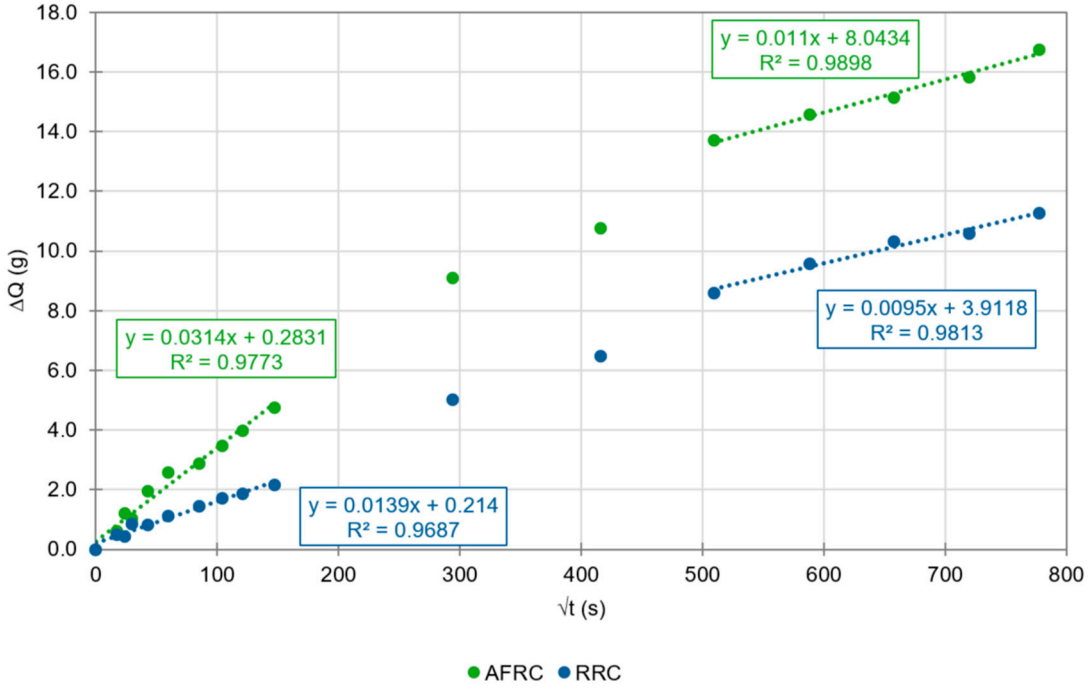

Figure 6. Curve of water absorption by capillary action.

Table 7. Capillary absorption coefficients (g/(m^2·s$^{0.5}$))

	Initial Absorption	Secondary Absorption
AFRC	3.14	1.10
RRC	1.39	0.95

Certainly, the sorptivity of AFRC is correlated to its porosity and the intrinsic absorption of the fibers, consistent with the findings discussed in the previous section. This represents an adverse outcome, as it would facilitate, through water, the transport of aggressive agents inside the matrix [76], potentially reaching the steel rebar and compromising durability. However, the results presented a tendency to decline over time. This may be associated with the hydrophilic properties of the fibers, which initially absorb water and, after reaching a saturated state, cease to absorb further water. At that point, the capillary effect primarily influences the pores within the concrete. This explains the similar behavior observed over a prolonged period, practically matching the RRC coefficient.

According to Bertolini et al. [77], the values obtained for the AFRC align with the classification of "good concrete" (classified by a w/c ratio < 0.50 and a compressive strength > 40 MPa). This indicates that, despite the increased absorption due to the presence of abaca fibers, their incorporation would not hinder the achievement of the necessary criteria for structural concrete, particularly in terms of capillary action. Thus, the use of AF in this context does not compromise the long-term performance of the concrete.

3.3.3. Chloride Ion Penetration

The capability of concrete to resist chloride ion penetration is correlated with the cumulative charge that flows across the specimens, measured in Coulombs. Figure 7 presents the mean value obtained from three different specimens tested for each mixture, conducted at 56 and 180 days, respectively, following the classification criteria specified in ASTM C1202-25.

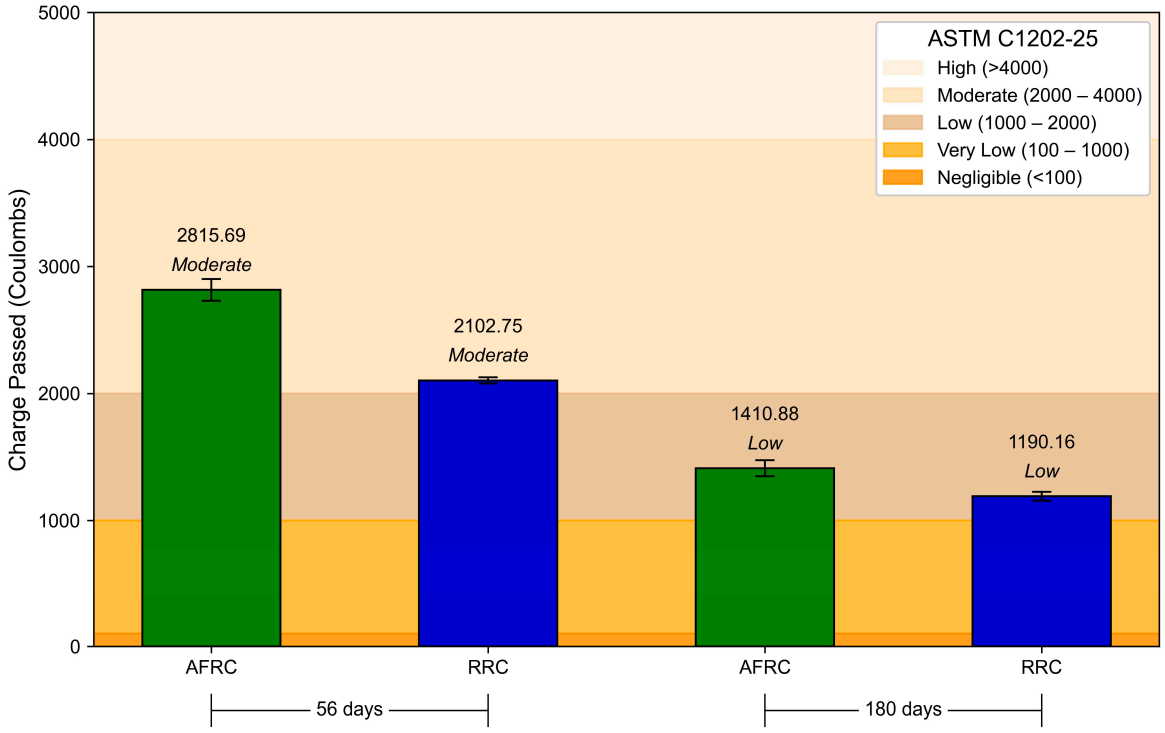

Figure 7. Chloride ion penetration, considering cumulative charge passed.

While the inclusion of fibers contributes to mitigating microcrack formation within the matrix, it can also lead to increased porosity, as demonstrated by the results outlined in the prior sections. In this context, the AFRC exhibited slightly lower resistance to chloride penetration compared to the RRC, admitting a higher electric charge of 33.94% at 56 days, which then decreased to 18.5% at 180 days. A similar trend was observed by Jamil et al. in their study incorporating jute fibers in concrete, which resulted in increased chloride penetration [78].

Furthermore, it has been established that, as the curing period increases, chloride penetration decreases [79]. This reduction is attributed to the modification of the pore structure of the hydrated cementitious system [80]. This trend was observed in the present study and is also supported by findings from other researchers [81,82]. Nevertheless, upon analyzing the total charge passed, the levels obtained remained within acceptable limits according to ASTM C1202-25 standards, indicating that AF did not significantly impair chloride resistance.

3.3.4. Carbonation Depth

Figure 8 illustrates the progression of CO_2 penetration, depicting the same specimen after 7 and 365 days in the accelerated carbonation chamber. Accordingly, Figure 9 presents the corresponding carbonation depth measurements over one year. It can be noticed in Figure 9 that there was a slight increase in the depth of carbonation of the AFRC. According to Zhuge et al. [83], natural fibers might act as bulk channels facilitating carbonation in

cement matrices. Additionally, the pore distribution in concrete is altered by the inherent morphology of NF, promoting carbon dioxide diffusion, thus increasing carbonation rate.

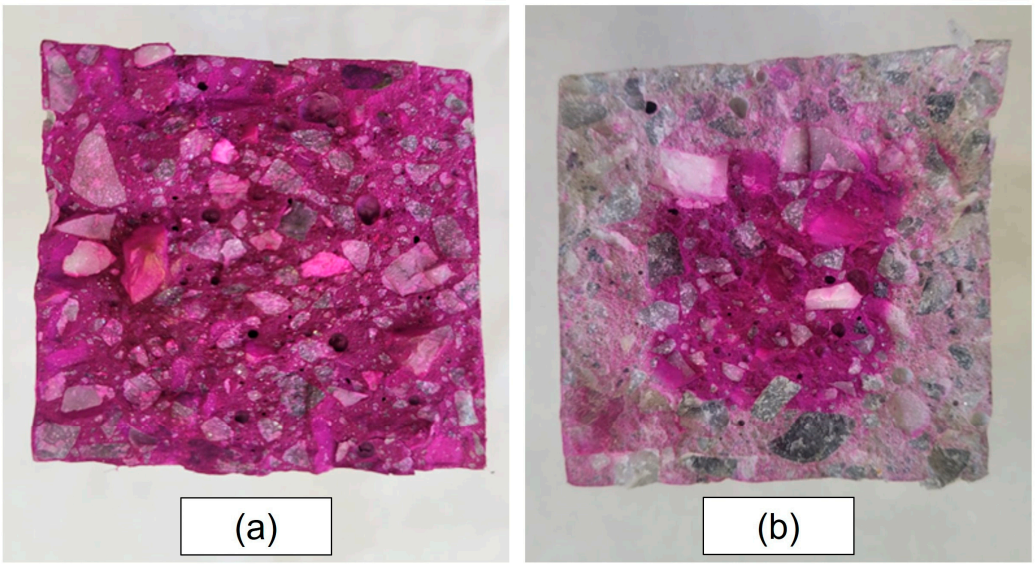

Figure 8. Progress of accelerated carbonation: (**a**) 7 days; (**b**) 365 days.

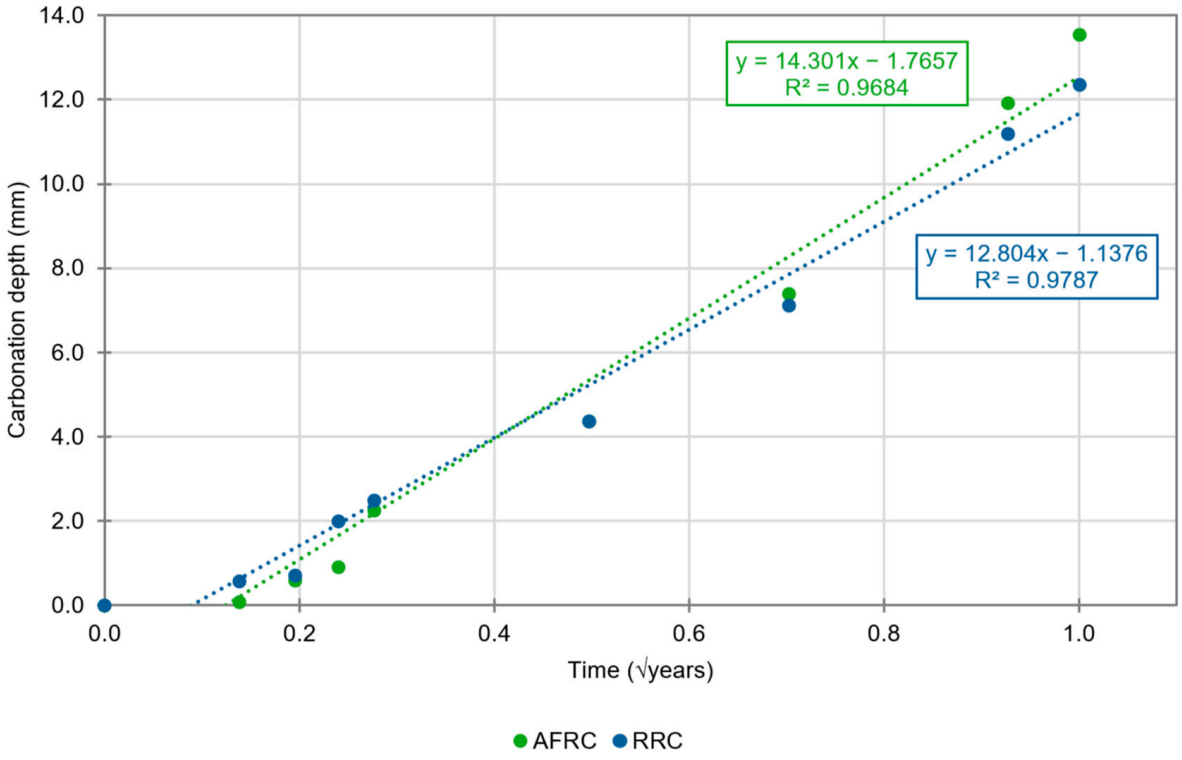

Figure 9. Evolution of accelerated carbonation depth as a square root of time.

Carbonation in concrete occurs as atmospheric carbon dioxide penetrates the material, reducing the pH by forming carbonates with alkali and calcium hydroxide in the hydrated cement phases [84]. While this process contributes to the hardening progress of concrete, it can negatively affect steel reinforcement. It is widely recognized that rebar is chemically protected when embedded in concrete, which is attributed to the passive film formation developed by steel in an alkaline environment. This passive film is impermeable, strongly adhered to the steel surface, and stable in the surrounding concrete mix, making corrosion

negligible. However, the pH reduction induced by the carbonation process leads to the loss of passivation in the steel, exposing the rebar to corrosion [77,85].

The time required for reinforcement depassivation can be estimated by extrapolating the accelerated carbonation depth to determine the coefficient under natural conditions. Following approaches adopted in prior studies [59,86] and applying the least squares method, the carbonation coefficients in the accelerated environment (Kc) were calculated as 14.30 for the AFRC and 12.80 for the RRC. These outcomes correspond to a carbon dioxide concentration of 1.0%, which is significantly higher than the 0.04% present in a natural environment. In line with previous studies [59,87], the carbonation coefficient was determined by considering the difference between the accelerated test concentration (sub-index c) and the real environmental concentration (sub-index r), estimated using the formula proposed by Gruyaert et al. [87]:

$$\frac{K_c}{K_r} = \frac{(x - x_0)_c}{(x - x_0)_r} = \sqrt{\frac{c_c}{c_r}} \quad (2)$$

where

K_c = accelerated test carbonation coefficient, mm/$\sqrt{}$year.
K_r = real-time carbonation coefficient, mm/$\sqrt{}$year.
C_c = accelerated test CO_2 concentration, percentage.
C_r = real environmental CO_2 concentration, percentage.

Consequently, the AFRC exhibited a *Kr* value of 2.86 mm/$\sqrt{}$year. Assuming "*t*" as time in years and "*d*" as distance, the equation $t = (d/Kr)^2$ can be applied to estimate the time needed for carbonation to reach a specific depth within the concrete, in accordance with the Spanish Code [32]. Based on a cover thickness of 30 mm, which corresponds to the minimum requirement for a 100-year projected service life in an environment with extreme natural carbonation (XC4) outlined in the Spanish Code, the initiation period for corrosion due to carbonation was estimated to be 110 years. Considering a typical propagation phase as proposed by Tuuti [88], the lifetime would extend 40 years further, resulting in a service life of 150 years for the AFRC, in contrast with 177 years for the RRC.

Moreover, these results highlight the influence of NF on carbonation, indicating the need for further durability-focused research on natural-fiber-reinforced concrete.

3.3.5. Direct Measurements of Corrosion Rate

The corrosion intensity was calculated as the mean of three independent measurements for each of the four specimens. Accordingly, to obtain a more reliable representation of the overall behavior, the final corrosion intensity for each week was calculated as the average of the four rebar specimens, as illustrated in Figure 10. This approach helps mitigate any potential variability attributable to the inherent nature of corrosion progression. As can be seen, during the first eight weeks, the corrosion intensity measurements remained within the passivation range, considering that the literature typically estimates its threshold around 0.10 $\mu A/cm^2$ [59,61,89]. Nevertheless, starting from week 19, the AFRC exhibited an increasing trend with a wider variation. Although fluctuations were observed, the general trend indicated a rise in corrosion intensity, surpassing the passivation threshold, and this pattern continued through the final measurement.

Based on the values obtained and supported by the previously discussed durability-related properties, the increase observed in corrosion can be attributed to the heterogeneity resulting from the presence of the fibers in the composite. The abaca fibers can increase the internal porosity of the concrete, as discussed previously, which in turn facilitates the ingress of aggressive agents such as CO_2 and moisture, accelerating the corrosion process. Additionally, the fiber deposition on the surface of the reinforcing steel creates a physical

interference between the cement paste and the rebar, affecting the fiber–matrix interface, potentially disrupting the passive film and reducing its protective efficiency.

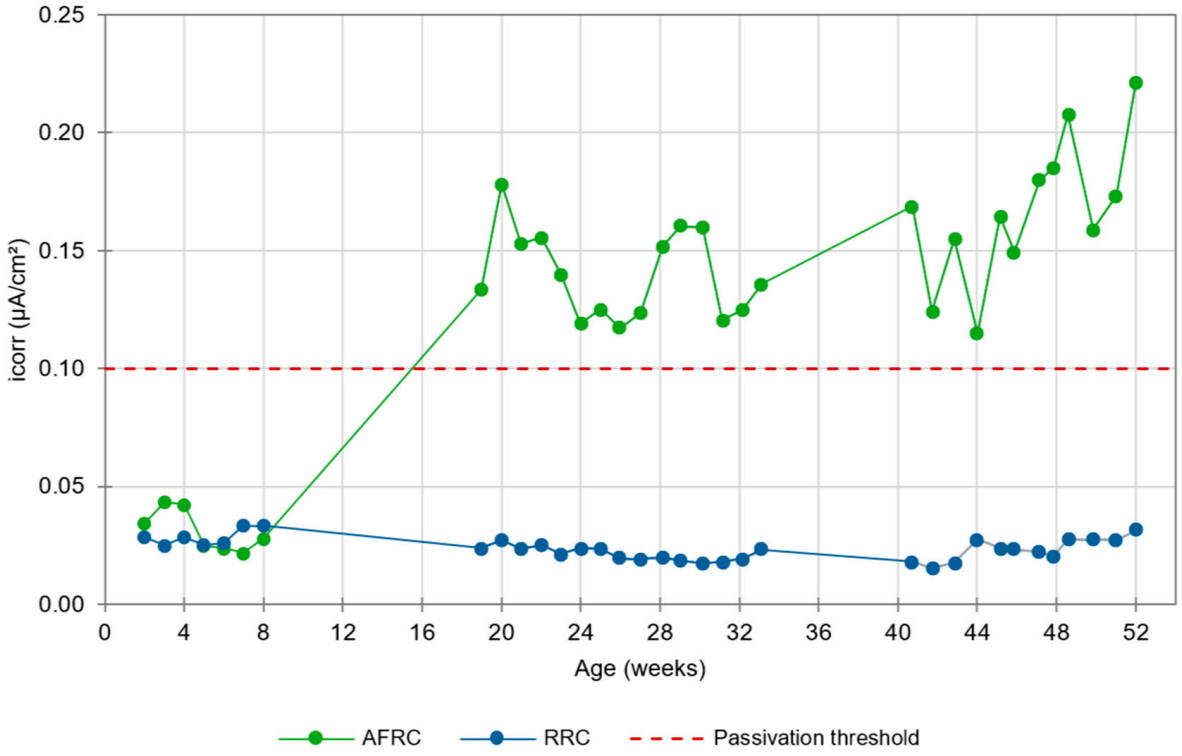

Figure 10. Evolution of steel rebar corrosion intensity.

To address the most critical scenario, the corrosion rate was evaluated from week 19, when the increase trend was detected, to the end of the study period. Considering this interval, the corrosion intensity obtained for the AFRC was 0.152 µA/cm^2, which was higher than that obtained for the RRC (0.022 µA/cm^2). Additionally, the velocity of corrosion for the AFRC was estimated, indicating a corresponding loss of steel of 1.76 µm/year [90]. To further refine the assessment of the impact of abaca fibers on the corrosion process, the service life was calculated utilizing the methodology outlined in the Spanish Code [32], considering the period time between the start of corrosion and the cover cracking, using the following formula [32]:

$$t_{corr} = \frac{80 \bullet c}{\emptyset \bullet v_{corr}} \quad (3)$$

where

t_{corr} = time from the initiation of corrosion to cover cracking, years.
c = concrete cover, mm.
$\emptyset$ = diameter of the rebar, mm.
v_{corr} = velocity of corrosion, µm/year.

Given the characteristics of the specimens prepared for this test and assuming that the observed corrosion trend continues, the service life for the AFRC is estimated to reach 113 years. Thus, as long as the surrounding concrete is not significantly altered by carbonation or chloride contamination, which could compromise the passive layer (as previously demonstrated in this study), durability in terms of steel corrosion would be ensured for this period.

Moreover, the findings indicate that the incorporation of AF led to an increase in corrosion intensity compared to that of the reference; however, no visible damage or significant deterioration was observed in the embedded rebar at this stage. This is illustrated in Figure 11, which presents cross-sectional images of both AFRC and RRC specimens.

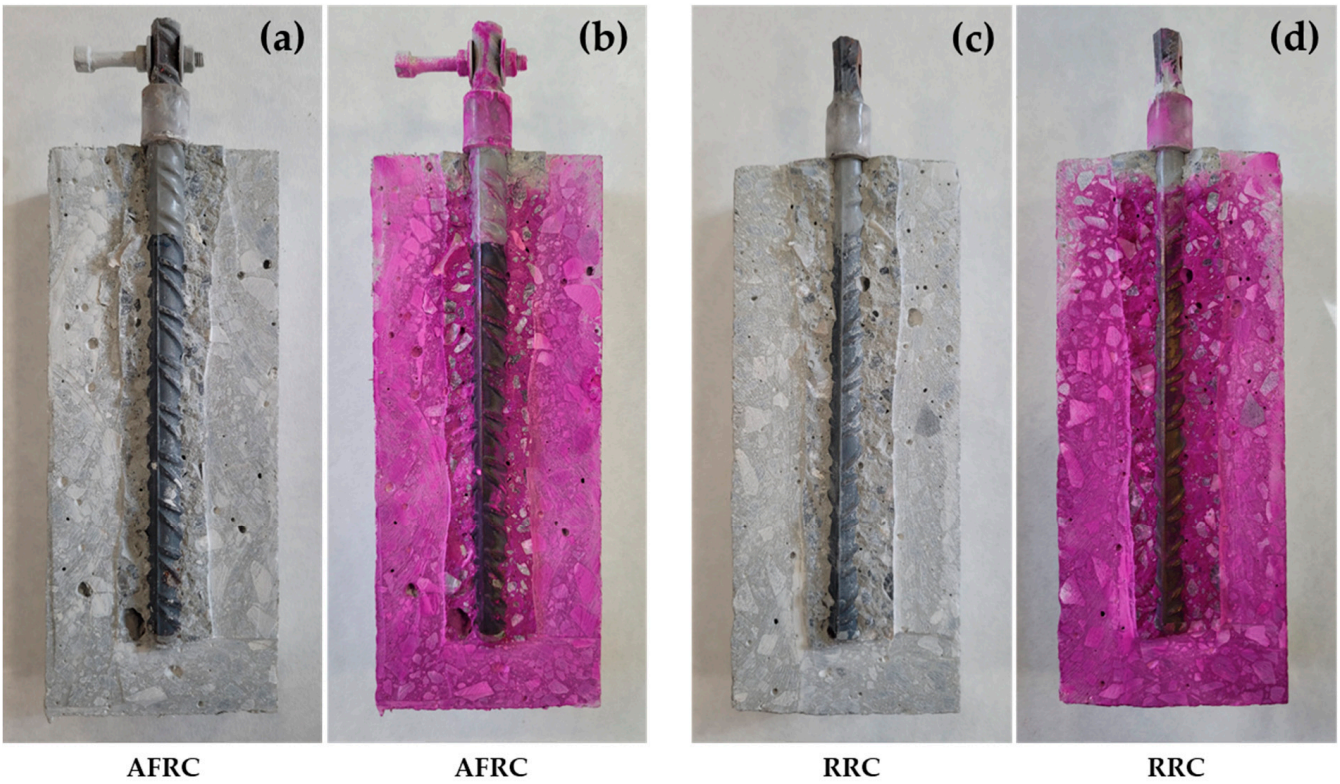

Figure 11. Cross-section images of the concrete specimens at the end of the test period, before and after the application of phenolphthalein solution: (**a**,**b**) AFRC, (**c**,**d**) RRC.

As depicted in Figure 11a,c, no visible signs of corrosion appeared in the steel reinforcement after one year of testing, and the phenolphthalein indicator demonstrated that the carbonation depth had not reached the rebar (Figure 11b,d). Nevertheless, while these outcomes offer initial insight into the effect of natural fibers on corrosion behavior, further studies are needed to fully determine their long-term implications.

4. Conclusions

This study evaluated the workability, mechanical, and durability-related properties of abaca-fiber-reinforced concrete, focusing on the influence of AF on these parameters. The results obtained led to the following conclusions:

(1) The fresh properties were not impaired by the presence of AF, preserving the workability and remaining within the required parameters of self-compacting concrete.
(2) AFRC demonstrated a significant 7.3% improvement in flexural strength by the incorporation of AF, while compressive strength was practically unaffected, only 1.8% lower than that of the reference concrete.
(3) A slight increase of 4.1% in porosity was observed in the AFRC, attributed to the incorporation of natural fibers, as these increase the presence of larger pores in the matrix. Similarly, due to the hydrophilic nature of AF, water absorption by capillary action increased initially but then decreased over time, reaching a negligible difference and virtually matching the coefficients.

(4) Regarding chloride penetration, the results showed minimal variation, with the presence of fibers having a slight impact but with values remaining within the classification indicated by the standard. Additionally, although the carbonation depth increased, as predicted by the porosity results, this rise did not prevent the AFRC from meeting the specified service life.
(5) The presence of AF notably influenced the corrosion intensity, resulting in higher and more unusual values. However, after estimating the service life, the AFRC still exceeded the 100-year period typically considered for most structures.

Considering these observations, the addition of abaca fibers generally resulted in an acceptable performance in both the fresh and hardened states of concrete. While the results suggest that AF holds potential as a reinforcement material, further investigation is necessary to confirm the long-term performance and to better understand their durability implications.

5. Future Research Directions

The outcomes and limitations of this research helped identify key areas requiring future research to further deepen the knowledge and understanding of natural-fiber-reinforced concrete, particularly that containing abaca fibers. In this regard, a main concern relates to the fiber–matrix interfacial transition zone, where material heterogeneity may have negative impacts on long-term durability. To evaluate this, further studies should employ microstructural analyses, including X-ray diffraction and mercury intrusion porosimetry, and deepen the exploration of SEM images. These techniques may reveal alterations in the pore structure, corrosion mechanisms, and incompatibility caused by the incorporation of fibers into the composite.

Moreover, to consider the utilization of NF in the field of structural concrete, advanced structural validations, such as fatigue and creep tests under cyclical and sustained loads, along with the assessment of damping properties related to energy dissipation, are recommended. Additionally, it is essential to consider the representativeness of laboratory testing, guaranteeing service life conditions that reproduce the complexity of real structural service conditions.

Finally, comparative evaluations of different industrial fibers (e.g., glass, polypropylene, and polyvinyl alcohol) will enable stronger comprehension in terms of performance, cost-effectiveness, and ecological implications. Following this approach, the incorporation of a life cycle assessment (LCA) will provide a quantitative evaluation of the environmental impact of AF, validating their feasible contribution to sustainable construction practices.

Author Contributions: Conceptualization, A.A.-M. and M.J.M.-E.; methodology, A.A.-M. and M.J.M.-E.; software, A.A.-M.; validation, A.A.-M. and M.J.M.-E.; formal analysis, A.A.-M.; investigation, A.A.-M. and S.A.-B.; resources, S.A.-B.; data curation, A.A.-M.; writing—original draft preparation, A.A.-M.; writing—review and editing, M.J.M.-E.; visualization, A.A.-M., S.A.-B. and M.J.M.-E.; supervision, M.J.M.-E.; project administration, M.J.M.-E. All authors have read and agreed to the published version of the manuscript.

Funding: This research received no external funding.

Data Availability Statement: The raw data supporting the conclusions of this article will be made available by the corresponding author on request.

Acknowledgments: The abaca fibers were supplied by Universidad Católica de Santiago de Guayaquil, for which the authors are grateful.

Conflicts of Interest: The authors declare no conflicts of interest.

Abbreviations

The following abbreviations are used in this manuscript:

NF	Natural fibers
AF	Abaca fibers
AFRC	Abaca-fiber-reinforced concrete
RRC	Reference reinforced concrete
FTIR	Fourier transform infrared spectroscopy
SEM	Scanning electron microscope
SCC	Self-compacting concrete
NS	Natural sand
NMG	Natural medium gravel
SP	Superplasticizer
SD	Standard deviation

References

1. Wang, Z.; Zuo, J.; Zhang, X.; Jiang, G.; Feng, L. Stress–Strain Behaviour of Hybrid-Fibre Engineered Cementitious Composite in Compression. *Adv. Cem. Res.* **2020**, *32*, 53–65. [CrossRef]
2. Geremew, A.; De Winne, P.; Demissie, T.A.; De Backer, H. Surface Modification of Bamboo Fibers through Alkaline Treatment: Morphological and Physical Characterization for Composite Reinforcement. *J. Eng. Fibers Fabr.* **2024**, *19*, 15589250241248764. [CrossRef]
3. Hassan, M.S. Moisture Sensitivity and Dimensional Stability of Carbonated Fibre–Cement Composites. *Adv. Cem. Res.* **2018**, *30*, 413–426. [CrossRef]
4. Benaimeche, O.; Carpinteri, A.; Mellas, M.; Ronchei, C.; Scorza, D.; Vantadori, S. The Influence of Date Palm Mesh Fibre Reinforcement on Flexural and Fracture Behaviour of a Cement-Based Mortar. *Compos. Part B Eng.* **2018**, *152*, 292–299. [CrossRef]
5. Contreras, C.; Albuja-Sánchez, J.; Proaño, O.; Ávila, C.; Damián-Chalán, A.; Peñaherrera-Aguirre, M. The Influence of Abaca Fiber Treated with Sodium Hydroxide on the Deformation Coefficients Cc, Cs, and Cv of Organic Soils. *Fibers* **2024**, *12*, 89. [CrossRef]
6. Bamaga, S.O. The Influence of Silica Fume on the Properties of Mortars Containing Date Palm Fibers. *Fibers* **2022**, *10*, 41. [CrossRef]
7. Luca, A.; Antonio, G.; Scalia Giada, L.; Fata Concetta Manuela, L.; Rosa, M. Life Cycle Assessment of a New Industrial Process for Sustainable Construction Materials. *Ecol. Indic.* **2023**, *148*, 110042. [CrossRef]
8. Anthony, R.; Suhalka, S.; Afsal, S.; Kumar, V.R.P. An Experimental Study on the Durability Properties of Abaca Fiber Concrete. *J. Eng. Res.* **2022**. [CrossRef]
9. Brandt, A.M. Fibre Reinforced Cement-Based (FRC) Composites after over 40 Years of Development in Building and Civil Engineering. *Compos. Struct.* **2008**, *86*, 3–9. [CrossRef]
10. Laverde, V.; Marin, A.; Benjumea, J.M.; Rincón Ortiz, M. Use of Vegetable Fibers as Reinforcements in Cement-Matrix Composite Materials: A Review. *Constr. Build. Mater.* **2022**, *340*, 127729. [CrossRef]
11. Bendahane, K.; Belkheir, M.; Mokaddem, A.; Doumi, B.; Boutaous, A. Date and Doum Palm Natural Fibers as Renewable Resource for Improving Interface Damage of Cement Composites Materials. *Beni-Suef Univ. J. Basic Appl. Sci.* **2023**, *12*, 37. [CrossRef]
12. Ferreira, S.R.; Pepe, M.; Martinelli, E.; de Andrade Silva, F.; Toledo Filho, R.D. Influence of Natural Fibers Characteristics on the Interface Mechanics with Cement Based Matrices. *Compos. Part B Eng.* **2018**, *140*, 183–196. [CrossRef]
13. Sadeghi, P.; Cao, Q.; Abouzeid, R.; Shayan, M.; Koo, M.; Wu, Q. Experimental and Statistical Investigations for Tensile Properties of Hemp Fibers. *Fibers* **2024**, *12*, 94. [CrossRef]
14. Doostkami, H.; Hernández-Figueirido, D.; Albero, V.; Piquer, A.; Serna, P.; Roig-Flores, M. Experimental Study on the Valorization of Rice Straw as Fiber for Concrete. *Fibers* **2025**, *13*, 28. [CrossRef]
15. Page, J.; Amziane, S.; Gomina, M.; Djelal, C.; Audonnet, F. Using Linseed Oil as Flax Fibre Coating for Fibre-Reinforced Cementitious Composite. *Ind. Crops Prod.* **2021**, *161*, 113168. [CrossRef]
16. Essaket, I.; El Wazna, M.; Azmami, O.; Sajid, L.; Allam, I.; El Maliki, A.; El Bouari, A.; Cherkaoui, O. Extraction and Chemical Treatments of Moroccan Sisal Fiber for Composite Applications. *Biomass Convers. Biorefin.* **2025**, *15*, 7077–7094. [CrossRef]
17. Kumar Sinha, A.; Narang, H.K.; Bhattacharya, S. Effect of Alkali Treatment on Surface Morphology of Abaca Fibre. *Mater. Today Proc.* **2017**, *4*, 8993–8996. [CrossRef]
18. Richter, S.; Stromann, K.; Müssig, J. Abacá (Musa Textilis) Grades and Their Properties—A Study of Reproducible Fibre Characterization and a Critical Evaluation of Existing Grading Systems. *Ind. Crops Prod.* **2013**, *42*, 601–612. [CrossRef]
19. Anthony, R.; Awasthi, S.Y.; Singh, P.; Prasath Kumar, V.R. An Experimental and Characteristic Study of Abaca Fiber Concrete. *IOP Conf. Ser. Mater. Sci. Eng.* **2020**, *912*, 032077. [CrossRef]

20. Tampi, R.; Parung, H.; Djamaluddin, R.; Amiruddin, A.A. Reinforced Concrete Mixture Using Abaca Fiber. *IOP Conf. Ser. Earth Environ. Sci.* **2020**, *419*, 012060. [CrossRef]
21. Thyavihalli Girijappa, Y.G.; Mavinkere Rangappa, S.; Parameswaranpillai, J.; Siengchin, S. Natural Fibers as Sustainable and Renewable Resource for Development of Eco-Friendly Composites: A Comprehensive Review. *Front. Mater.* **2019**, *6*, 226. [CrossRef]
22. Alcivar-Bastidas, S.; Petroche, D.M.; Ramirez, A.D.; Martinez-Echevarria, M.J. Characterization and Life Cycle Assessment of Alkali Treated Abaca Fibers: The Effect of Reusing Sodium Hydroxide. *Constr. Build. Mater.* **2024**, *449*, 138522. [CrossRef]
23. Arvizu-Montes, A.; Martinez-Echevarria, M.J. Vegetable Fibers in Cement Composites: A Bibliometric Analysis, Current Status, and Future Outlooks. *Materials* **2025**, *18*, 333. [CrossRef]
24. Kabir, M.M.; Wang, H.; Lau, K.T.; Cardona, F. Chemical Treatments on Plant-Based Natural Fibre Reinforced Polymer Composites: An Overview. *Compos. Part B Eng.* **2012**, *43*, 2883–2892. [CrossRef]
25. Achour, A.; Ghomari, F.; Belayachi, N. Properties of Cementitious Mortars Reinforced with Natural Fibers. *J. Adhes. Sci. Technol.* **2017**, *31*, 1938–1962. [CrossRef]
26. Boulos, L.; Foruzanmehr, M.R.; Tagnit-Hamou, A.; Robert, M. The Effect of a Zirconium Dioxide Sol-Gel Treatment on the Durability of Flax Reinforcements in Cementitious Composites. *Cem. Concr. Res.* **2019**, *115*, 105–115. [CrossRef]
27. Jiang, D.; An, P.; Cui, S.; Xu, F.; Tuo, T.; Zhang, J.; Jiang, H. Effect of Leaf Fiber Modification Methods on Mechanical and Heat-Insulating Properties of Leaf Fiber Cement-Based Composite Materials. *J. Build. Eng.* **2018**, *19*, 573–583. [CrossRef]
28. Elbehiry, A.; Elnawawy, O.; Kassem, M.; Zaher, A.; Uddin, N.; Mostafa, M. Performance of Concrete Beams Reinforced Using Banana Fiber Bars. *Case Stud. Constr. Mater.* **2020**, *13*, e00361. [CrossRef]
29. Martinez-Echevarria, M.J.; Lopez-Alonso, M.; Cantero Romero, D.; Rodríguez Montero, J. Influence of the Previous State of Corrosion of Rebars in Predicting the Service Life of Reinforced Concrete Structures. *Constr. Build. Mater.* **2018**, *188*, 915–923. [CrossRef]
30. Berrocal, C.G.; Löfgren, I.; Lundgren, K.; Tang, L. Corrosion Initiation in Cracked Fibre Reinforced Concrete: Influence of Crack Width, Fibre Type and Loading Conditions. *Corros. Sci.* **2015**, *98*, 128–139. [CrossRef]
31. Zhao, X.; Liu, R.; Qi, W.; Yang, Y. Corrosion Resistance of Concrete Reinforced by Zinc Phosphate Pretreated Steel Fiber in the Presence of Chloride Ions. *Materials* **2020**, *13*, 3636. [CrossRef] [PubMed]
32. Ministerio de Transportes y Movilidad Sostenible. *Código Estructural, Agencia Estatal. Boletín Oficial del Estado*; Ministerio de Transportes y Movilidad Sostenible: Madrid, Spain, 2021.
33. Elsaid, A.; Dawood, M.; Seracino, R.; Bobko, C. Mechanical Properties of Kenaf Fiber Reinforced Concrete. *Constr. Build. Mater.* **2011**, *25*, 1991–2001. [CrossRef]
34. Ardanuy, M.; Claramunt, J.; Toledo Filho, R.D. Cellulosic Fiber Reinforced Cement-Based Composites: A Review of Recent Research. *Constr. Build. Mater.* **2015**, *79*, 115–128. [CrossRef]
35. Alcivar-Bastidas, S.; Petroche, D.M.; Martinez-Echevarria, M.J. The Effect of Different Treatments on Abaca Fibers Used in Cementitious Composites. *J. Nat. Fibers* **2023**, *20*, 2177235. [CrossRef]
36. Cai, M.; Takagi, H.; Nakagaito, A.N.; Katoh, M.; Ueki, T.; Waterhouse, G.I.N.; Li, Y. Influence of Alkali Treatment on Internal Microstructure and Tensile Properties of Abaca Fibers. *Ind. Crops Prod.* **2015**, *65*, 27–35. [CrossRef]
37. Mayakun, J.; Klinkosum, P.; Chaichanasongkram, T.; Sarak, S.; Kaewtatip, K. Characterization of a New Natural Cellulose Fiber from Enhalus Acoroides and Its Potential Application. *Ind. Crops Prod.* **2022**, *186*, 115285. [CrossRef]
38. Rashidi, O.; Abdulkhani, A.; Hejazi, S.; Ashori, A.; Hosseinzadeh, J.; Sun, F. Preparation and Characterization of Cellulose from Wheat Straw Using Formic/Acetic Acid Pulping and Cu-Activated Hydrogen Peroxide Bleaching. *Cellulose* **2025**, *32*, 165–185. [CrossRef]
39. Marvila, M.T.; Azevedo, A.R.G.; Cecchin, D.; Costa, J.M.; Xavier, G.C.; De Fátima Do Carmo, D.; Monteiro, S.N. Durability of Coating Mortars Containing Açaí Fibers. *Case Stud. Constr. Mater.* **2020**, *13*, e00406. [CrossRef]
40. Rai, P.S.; Unnikrishnan, S.; Chandrashekar, A. Influence of Alkali Treatment on Physiochemical and Morphological Properties of Palmyra Fibers. *Ind. Crops Prod.* **2025**, *224*, 120298. [CrossRef]
41. Okamura, H.; Ouchi, M. Self-Compacting Concrete. *ACT* **2003**, *1*, 5–15. [CrossRef]
42. *EUNE-EN 197-1*; Cement. Part 1: Composition, Specifications and Conformity Criteria for Common Cements. European Committee for Standarization: Madrid, Spain, 2011.
43. Shah, V.; Parashar, A.; Mishra, G.; Medepalli, S.; Krishnan, S.; Bishnoi, S. Influence of Cement Replacement by Limestone Calcined Clay Pozzolan on the Engineering Properties of Mortar and Concrete. *Adv. Cem. Res.* **2020**, *32*, 101–111. [CrossRef]
44. Koura, B.-I.O.; Hosseinpoor, M.; Yahia, A. Coupled Effect of Fine Mortar and Granular Skeleton Characteristics on Dynamic Stability of Self-Consolidating Concrete as a Diphasic Material. *Constr. Build. Mater.* **2020**, *263*, 120131. [CrossRef]
45. Patil, S.; Bhaskar, R.; Xavier, J.R. Optimization of Rheological and Mechanical Properties of Sustainable Lateritic Self-Compacting Concrete Containing Sisal Fiber Using Response Surface Methodology. *J. Build. Eng.* **2024**, *84*, 108574. [CrossRef]

46. *UNE-EN 12350-8*; Testing Fresh Concrete. Part 8: Self-Compacting Concrete. Slump-Flow Test. European Committee for Standarization: Madrid, Spain, 2020.
47. *UNE-EN 12350-9*; Testing Fresh Concrete. Part 9: Self-Compacting Concrete. V-Funnel Test. European Committee for Standarization: Madrid, Spain, 2011.
48. *UNE-EN 12350-12*; Testing Fresh Concrete. Part 12: Self-Compacting Concrete. J-Ring Test. European Committee for Standarization: Madrid, Spain, 2011.
49. *UNE-EN 12350-10*; Testing Fresh Concrete. Part 10: Self-Compacting Concrete. L Box Test. European Committee for Standarization: Madrid, Spain, 2011.
50. *UNE-EN 12390-3*; Testing Hardened Concrete. Part 3: Compressive Strength of Test Specimens. European Committee for Standarization: Madrid, Spain, 2020.
51. *UNE-EN 12390-5*; Testing Hardened Concrete. Part 5: Flexural Strength of Test Specimens. European Committee for Standarization: Madrid, Spain, 2020.
52. Pan, T. Continuous Damage of Concrete Structures Due to Reinforcement Corrosion: A Micromechanical and Multi-Physics Based Analysis. *J. Build. Eng.* **2024**, *95*, 110139. [CrossRef]
53. Guo, R.; Guo, Z.; Yao, G.; Jin, Y.; Liu, Z. Hybrid Prediction Model for Reinforcements' Corrosion Stage by Multiple Nondestructive Electrochemical Indices. *J. Build. Eng.* **2024**, *82*, 108327. [CrossRef]
54. *UNE 83980*; Concrete Durability. Test Methods. Determination of the Water Absorption, Density and Accessible Porosity for Water in Concrete. ANEFHOP: Madrid, Spain, 2014.
55. *UNE 83982*; Concrete Durability. Test Methods. Determination of the Capillary Suction in Hardened Concrete. Fagerlund Method. ANEFHOP: Madrid, Spain, 2008.
56. *ASTM C1202-25*; Standard Test Method for Electrical Indication of Concrete's Ability to Resist Chloride Ion Penetration. ASTM: West Conshohocken, PA, USA, 2025.
57. *UNE-EN 12390-12*; Testing Hardened Concrete. Part 12: Determination of the Carbonation Resistance of Concrete. Accelerated Carbonation Method. European Committee for Standarization: Madrid, Spain, 2020.
58. Stern, M.; Geary, A.L. Electrochemical Polarization: I. A Theoretical Analysis of the Shape of Polarization Curves. *J. Electrochem. Soc.* **1957**, *104*, 56. [CrossRef]
59. Martinez-Echevarria, M.J.; Del Castillo, J.P.; Rodríguez Montero, J.; López-Alonso, M. Reinforcement Corrosion in Self-Compacting Concrete Made with Waste Filler of Bituminous Mixtures. *Constr. Build. Mater.* **2024**, *411*, 134623. [CrossRef]
60. Avila-Mendoza, J.; Flores, J.M.; Castillo, U.C. Effect of Superficial Oxides on Corrosion of Steel Reinforcement Embedded in Concrete. *Corrosion* **1994**, *50*, 879–885. [CrossRef]
61. González, J.A.; Ramírez, E.; Bautista, A.; Feliu, S. The Behaviour of Pre-Rusted Steel in Concrete. *Cem. Concr. Res.* **1996**, *26*, 501–511. [CrossRef]
62. El-Dieb, A.S.; Reda Taha, M.M. Flow Characteristics and Acceptance Criteria of Fiber-Reinforced Self-Compacted Concrete (FR-SCC). *Constr. Build. Mater.* **2012**, *27*, 585–596. [CrossRef]
63. Grzesiak, S.; Pahn, M.; Schultz-Cornelius, M.; Harenberg, S.; Hahn, C. Influence of Fiber Addition on the Properties of High-Performance Concrete. *Materials* **2021**, *14*, 3736. [CrossRef] [PubMed]
64. Derdour, D.; Behim, M.; Benzerara, M. Effect of Date Palm and Polypropylene Fibers on the Characteristics of Self-Compacting Concretes: Comparative Study. *Frat. Integrità Strutt.* **2023**, *17*, 31–50. [CrossRef]
65. García, G.; Cabrera, R.; Rolón, J.; Pichardo, R.; Thomas, C. Natural Fibers as Reinforcement of Mortar and Concrete: A Systematic Review from Central and South American Regions. *J. Build. Eng.* **2024**, *98*, 111267. [CrossRef]
66. Da Fonseca, R.P.; Rocha, J.C.; Cheriaf, M. Mechanical Properties of Mortars Reinforced with Amazon Rainforest Natural Fibers. *Materials* **2020**, *14*, 155. [CrossRef] [PubMed]
67. Ortiz-Lozano, J.A.; De La Fuente-Antequera, A.; Segura-Pérez, I.; Aguado De Cea, A.; Parapinski Dos Santos, A.C.; Pacheco-Martinez, J.; Soto-Bernal, J.J. Characterization of a Fibre-Reinforced Selfcompacting Concrete with 100% of Mixed Recycled Aggregates. *Int. J. CMEM* **2017**, *6*, 584–593. [CrossRef]
68. Martín, J.; Rodríguez Montero, J.; Moreno, F.; Piqueras Sala, J.L.; Rubio, M.C. Feasibility Analysis of the Reuse of Waste Filler of Bituminous Mixtures for the Production of Self-Compacting Concrete. *Mater. Des.* **2013**, *46*, 372–380. [CrossRef]
69. Rajkohila, A.; Chandar, S.P.; Ravichandran, P.T. Flexural Performance of HSC Beams Containing Natural Fibers. *J. Build. Rehabil.* **2024**, *9*, 71. [CrossRef]
70. Lamichhane, N.; Lamichhane, A.; Gyawali, T.R. Enhancing Mechanical Properties of Mortar with Short and Thin Banana Fibers: A Sustainable Alternative to Synthetic Fibers. *Heliyon* **2024**, *10*, e30652. [CrossRef]
71. Karahan, O.; Atiş, C.D. The Durability Properties of Polypropylene Fiber Reinforced Fly Ash Concrete. *Mater. Des.* **2011**, *32*, 1044–1049. [CrossRef]
72. Wu, Z.; Wang, X.; Chen, Z. Experimental Study on Preparation and Performance of the Corn Straw Fiber (CSF) Reinforced EPS Concrete. *J. Build. Eng.* **2024**, *89*, 109378. [CrossRef]

73. Assié, S.; Escadeillas, G.; Waller, V. Estimates of Self-Compacting Concrete 'Potential' Durability. *Constr. Build. Mater.* **2007**, *21*, 1909–1917. [CrossRef]
74. Valcuende, M.; Parra, C. Natural Carbonation of Self-Compacting Concretes. *Constr. Build. Mater.* **2010**, *24*, 848–853. [CrossRef]
75. Caixeta Silva, T.R.; Silva De Aquino, L.A.; Mesquita, L.C.; Marques, M.G.; De Azevedo, A.R.G.; Marvila, M.T. Innovative Cementitious Composites Produced with Corn Straw Fiber: Effect of the Alkaline Treatments. *Appl. Sci.* **2024**, *14*, 11117. [CrossRef]
76. Shan, H.; Xu, J.; Jiang, L.; Wang, Z. Improvement of Mortar Durability by Electrochemical Technique. *Adv. Cem. Res.* **2017**, *29*, 429–437. [CrossRef]
77. Bertolini, L.; Elsener, B.; Pedeferri, P.; Polder, R.B. *Corrosion of Steel in Concrete: Prevention, Diagnosis, Repair*, 1st ed.; Wiley: Hoboken, NJ, USA, 2003; ISBN 978-3-527-30800-2.
78. Jamil, K.; Shabbir, F.; Raza, A. Performance Evaluation of Jute Fiber-reinforced Recycled Aggregate Concrete: Strength and Durability Aspects. *Struct. Concr.* **2023**, *24*, 6520–6538. [CrossRef]
79. Pandey, A.; Kumar, B. Evaluation of Water Absorption and Chloride Ion Penetration of Rice Straw Ash and Microsilica Admixed Pavement Quality Concrete. *Heliyon* **2019**, *5*, e02256. [CrossRef]
80. Ramezanianpour, A.A.; Malhotra, V.M. Effect of Curing on the Compressive Strength, Resistance to Chloride-Ion Penetration and Porosity of Concretes Incorporating Slag, Fly Ash or Silica Fume. *Cem. Concr. Compos.* **1995**, *17*, 125–133. [CrossRef]
81. Gesoğlu, M.; Güneyisi, E. Strength Development and Chloride Penetration in Rubberized Concretes with and without Silica Fume. *Mater. Struct.* **2007**, *40*, 953–964. [CrossRef]
82. Momeen Ul Islam, M.; Li, J.; Roychand, R.; Saberian, M. Investigation of Durability Properties for Structural Lightweight Concrete with Discarded Vehicle Tire Rubbers: A Study for the Complete Replacement of Conventional Coarse Aggregates. *Constr. Build. Mater.* **2023**, *369*, 130634. [CrossRef]
83. Zhuge, Y.; Ong, P.B.; Wong, H.S.; Myers, R.J. Natural Fibre-Enhanced CO_2 Transport and Uptake in Cement Pastes Subjected to Enforced Carbonation. *J. CO2 Util.* **2024**, *90*, 102983. [CrossRef]
84. Andrade, C. Evaluation of the Degree of Carbonation of Concretes in Three Environments. *Constr. Build. Mater.* **2020**, *230*, 116804. [CrossRef]
85. Criado, M. The Corrosion Behaviour of Reinforced Steel Embedded in Alkali-Activated Mortar. In *Handbook of Alkali-Activated Cements, Mortars and Concretes*; Elsevier: Amsterdam, The Netherlands, 2015; pp. 333–372, ISBN 978-1-78242-276-1.
86. Esquinas, A.R.; Álvarez, J.I.; Jiménez, J.R.; Fernández, J.M. Durability of Self-Compacting Concrete Made from Non-Conforming Fly Ash from Coal-Fired Power Plants. *Constr. Build. Mater.* **2018**, *189*, 993–1006. [CrossRef]
87. Gruyaert, E.; Van Den Heede, P.; De Belie, N. Carbonation of Slag Concrete: Effect of the Cement Replacement Level and Curing on the Carbonation Coefficient—Effect of Carbonation on the Pore Structure. *Cem. Concr. Compos.* **2013**, *35*, 39–48. [CrossRef]
88. Tuutti, K. *Corrosion of Steel in Concrete*; Swedish Cement and Concrete Research Institute: Stockholm, Sweden, 1982.
89. Andrade, C.; Alonso, C.; González, J. Some Laboratory Experiments on the Inhibitor Effect of Sodium Nitrite on Reinforcement Corrosion. *Cem. Concr. Aggr.* **1986**, *8*, 110. [CrossRef]
90. Garcés Terradillos, P. *Recomendaciones Técnicas*; Alconpat Internacional: Mérida, Mexico, 2020.